Cardiovascular Research (2015) **107**, 216–225
doi:10.1093/cvr/cvv156

Nebulette knockout mice have normal cardiac function, but show Z-line widening and up-regulation of cardiac stress markers

Giuseppina Mastrototaro[1,2†], Xingqun Liang[3†‡], Xiaodong Li[3¶], Pierluigi Carullo[1,4], Nicoletta Piroddi[5], Chiara Tesi[5], Yusu Gu[3], Nancy D. Dalton[3], Kirk L. Peterson[3], Corrado Poggesi[5], Farah Sheikh[3], Ju Chen[3]*, and Marie-Louise Bang[1,4§]*

[1]Humanitas Clinical and Research Center, Via Manzoni 113, 20089 Rozzano, Milan, Italy; [2]University of Milano-Bicocca, Milan, Italy; [3]Department of Medicine, University of California San Diego, 9500 Gilman Drive, La Jolla, CA 92093-0613C, USA; [4]Institute of Genetic and Biomedical Research, UOS Milan, National Research Council, Milan, Italy; and [5]Department of Experimental and Clinical Medicine, University of Florence, Florence, Italy

Received 1 January 2015; revised 15 April 2015; accepted 26 April 2015; online publish-ahead-of-print 18 May 2015

Time for primary review: 58 days

Aims Nebulette is a 109 kDa modular protein localized in the sarcomeric Z-line of the heart. *In vitro* studies have suggested a role of nebulette in stabilizing the thin filament, and missense mutations in the *nebulette* gene were recently shown to be causative for dilated cardiomyopathy and endocardial fibroelastosis in human and mice. However, the role of nebulette *in vivo* has remained elusive. To provide insights into the function of nebulette *in vivo*, we generated and studied nebulette-deficient ($nebl^{-/-}$) mice.

Methods and results $Nebl^{-/-}$ mice were generated by replacement of exon 1 by Cre under the control of the endogenous *nebulette* promoter, allowing for lineage analysis using the ROSA26 Cre reporter strain. This revealed specific expression of nebulette in the heart, consistent with *in situ* hybridization results. $Nebl^{-/-}$ mice exhibited normal cardiac function both under basal conditions and in response to transaortic constriction as assessed by echocardiography and haemodynamic analyses. Furthermore, histological, IF, and western blot analysis showed no cardiac abnormalities in $nebl^{-/-}$ mice up to 8 months of age. In contrast, transmission electron microscopy showed Z-line widening starting from 5 months of age, suggesting that nebulette is important for the integrity of the Z-line. Furthermore, up-regulation of cardiac stress responsive genes suggests the presence of chronic cardiac stress in $nebl^{-/-}$ mice.

Conclusion Nebulette is dispensable for normal cardiac function, although Z-line widening and up-regulation of cardiac stress markers were found in $nebl^{-/-}$ heart. These results suggest that the *nebulette* disease causing mutations have dominant gain-of-function effects.

Keywords Heart • Sarcomere • Z-line • Knockout mice • Dilated cardiomyopathy

1. Introduction

Nebulette is a 109 kDa cardiac-specific sarcomeric protein, highly homologous to the C-terminal Z-disc region of the larger protein nebulin (~500–900 kDa), which is predominantly expressed in skeletal muscle.[1] Like nebulin, nebulette is composed of 35-residue nebulin-like repeats, a serine-rich region, and a C-terminal SH3 domain.[2] However, whereas nebulin contains up to 185 nebulin-like re-

* Corresponding authors. Tel: +1 858 8224276; fax: +1 858 8223027. Email: juchen@ucsd.edu (J.C.); Tel: +39 0282245210; fax: +39 0282245290. Email: marie-louise.bang@cnr.it (M.-L.B.).
† G.M. and X.L. equally contributed to the work.
‡ Present address. Key Laboratory of Arrhythmia, Ministry of Education, East Hospital, Tongji University School of Medicine, Shanghai 200120, China.
¶ Present address. Department of Pathology, Keck Medical School, University of Southern California, Los Angeles, CA, USA.
§ M.L.B. will handle correspondence during refereeing and publication.

peats and extends from the Z-line along the length of the thin filament, nebulette contains only up to 23 repeats and is localized at the Z-line from which it protrudes only a short distance along the thin filament.[2] The nebulin-like repeats of both nebulin and nebulette bind to the thin filament components actin,[3–6] tropomyosin 1,[4,5,7–10] and troponin T,[5,9] while their C-terminal SH3 domains have been reported to interact with myopalladin,[11] palladin,[11] α-actinin,[4] zyxin,[12] N-WASP,[13] and titin's Zis1 and PEVK regions[14–16] in the Z-disc. Additionally, nebulette binds to filamin C[8] and possibly Cypher/ZASP,[8] whereas nebulin C-terminal repeats M160–164 were reported to interact with CapZ[17] and desmin.[18,19] It remains to be determined whether nebulette can also interact with CapZ and desmin. Based on its interaction with thin filament components and close connection to the actin filament along its length, nebulin was long thought to be a ruler regulating thin filament length.[1,20] However, recent findings by us and others have revealed that it does not directly regulate thin filament length, but rather stabilizes the thin filament, allowing it reach its final length.[17,21–23] Although nebulette is localized in the Z-line and does not extend the length of the thin filament, loss of endogenous nebulette in chicken embryonic cardiomyocytes as a result of overexpression of the nebulette serine-rich region and/or SH3 domain resulted in shorter thin filaments,[24] similar to observations in skeletal muscle of nebulin knockout (KO) mice.[16,21] Thus, despite of its localization in the Z-line, also nebulette appears to play a role in stabilizing the thin filament. Furthermore, consistent with the finding that nebulette repeats increase the affinity of the tropomyosin–troponin T complex for F-actin,[5] loss of nebulette was reported to cause a reduction in tropomyosin and troponin T staining along the thin filament without affecting the organization of the Z-line or the thick filament.[7,24] The role of nebulette in the Z-line remains elusive, but based on its high homology with the C-terminal Z-line region of nebulin, the two proteins are thought to play similar roles in the Z-line. Nebulin KO mice exhibit widened and misaligned Z-lines,[16,21,25] suggesting a role of nebulin in the maintenance of Z-line width and the lateral registration of Z-lines, likely through its binding to desmin.[21,25] Furthermore, we recently showed that mice deficient for the nebulin SH3 domain are more susceptible to eccentric contraction-induced injury,[26] consistent with a role of nebulin in maintaining Z-line structure during load, protecting the muscle from injury. The recent identification of *nebulette* variants in patients with dilated cardiomyopathy (DCM) and endocardial fibroelastosis[27] suggests that nebulette may play a similar important role in the heart. The identified variants include four heterozygous missense mutations localized within different regions of the *nebulette* gene, associated with DCM of different severity and age of disease onset. The K60N, Q128R, and G202R variants reside in the nebulin-like repeat region in the I-band region, whereas the A592E variant is localized in the Z-line region. The patients carrying the Q128R and A592 variants (the patient carrying the A582 variant also carried a mutation in α-actinin 2) were affected from birth, whereas the patients carrying the K60N and G202R variants developed adult-onset DCM. The cardiomyopathy phenotype was recapitulated in transgenic mouse models overexpressing nebulette mutations, resulting in various phenotypes ranging from embryonic lethality (K60N and Q128R) to adult-onset progressive DCM (G202R and A592E) associated with disruption of I-band and Z-line proteins.[27,28] To provide new insights into the function of nebulette in the heart *in vivo*, we generated and studied nebulette-deficient ($nebl^{-/-}$) mice. Surprisingly, $nebl^{-/-}$ mice exhibited normal cardiac function, although Z-line widening and up-regulation of markers associated with cardiac stress were observed.

2. Methods

2.1 Generation of nebulette KO mice

Nebulette genomic DNA was isolated from a 129SVJ mouse genomic library (Stratagene, La Jolla, CA, USA) and used to generate a nebulette-targeting construct for the replacement of nebulette exon 1 by a cre-FRT-neo-FRT cassette under the control of the endogenous *nebulette* promoter essentially as described previously (*Figure 1A*).[21] The targeting construct was verified by sequencing and linearized with *Not*I before electroporation into R1 embryonic stem cells at the Transgenic Core Facility at the University of California, San Diego. G418-resistant ES clones were screened for homologous recombination by *Bam*HI digestion of ES cell DNA and Southern blot analysis with the probe shown in *Figure 1B*. G418-resistant ES clones were screened for homologous recombination by Southern blot analysis with the probe shown in *Figure 1B*. The wild-type (WT) allele is represented by the band of 8.5 kb, whereas the 5.4 kb band represents the correctly targeted mutant allele. Cells from two independent homologous recombinant ES clones were microinjected into C57BL/6

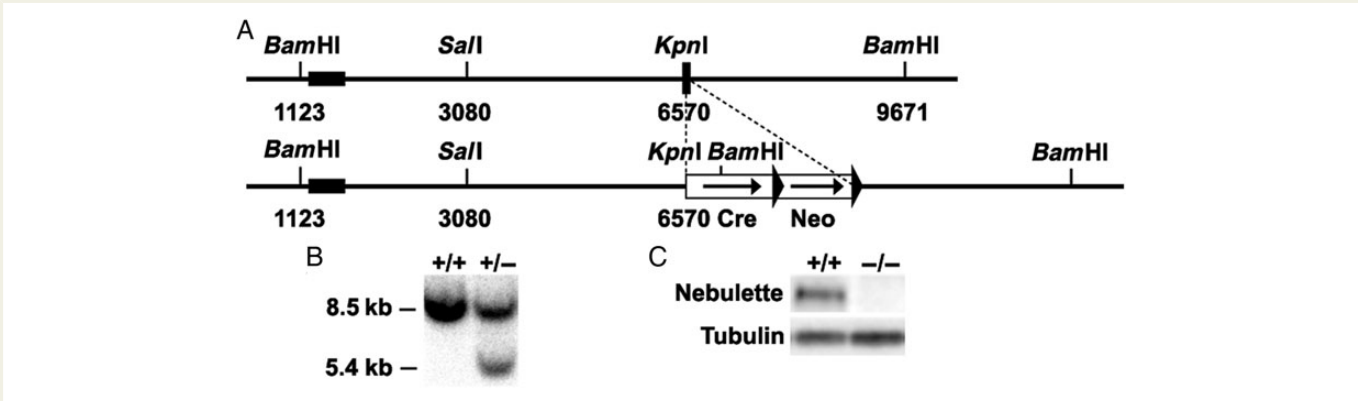

Figure 1 Targeting of the *nebulette* gene. (*A*) Targeting strategy for generation of nebulette KO ($nebl^{-/-}$) mice. A restriction map of the relevant genomic region of *nebulette* is shown on top and the mutated locus after recombination is shown at the bottom. The black box indicates exon 1 and arrows indicate frt sites. Neo, neomycin-resistance gene. (*B*) Detection of WT and targeted alleles by Southern blot analysis after digestion with *Bam*HI using the probe shown in *A*. (*C*) Detection of nebulette protein by western blot analysis. α-Tubulin antibody was used as a loading control.

blastocysts and transferred into pseudopregnant mice. Male chimeras resulting from the microinjections were bred with female Black Swiss mice to generate germline-transmitted heterozygous nebulette KO mice (*nebl*$^{+/-}$), which were subsequently intercrossed to generate homozygous KO mice (*nebl*$^{-/-}$). Offspring from intercrosses were genotyped by PCR analysis using mouse tail DNA and WT (sense: GTGCCCCAGA GACTTGGTAG; reverse: AGAGGGAGGGAGAAGGTCTG), and mutant allele-specific primers (sense: GTTCGCAAGAACCTGATGCACA; reverse: CTAGAGCCTGTTTTGCACGTTC). Successful ablation of the nebulette gene was confirmed by western blot analysis using polyclonal antibodies against nebulette (kindly provided by Dr Siegfried Labeit, Medical Faculty Mannheim, University of Heidelberg, Germany). All animal studies were approved by the University of California San Diego Animal Care and Use Committee and the Italian Ministry of Health. Animal procedures were performed in full compliance with the guidelines for the Guide for the Care and Use of Laboratory Animals, eighth edition (2011), published by the US National Institutes of Health (NIH) and the Directive 2010/63/EU of the European Parliament on the protection of animals use for scientific purposes. Mice for experiments were sacrificed by cervical dislocation following anaesthesia by an intraperitoneal injection of a mixture of ketamine (100 mg/kg) and xylazine (5 mg/kg).

2.2 β-Galactosidase staining

To perform fate mapping of nebulette-expressing cells, *nebl*$^{+/-}$ mice were crossed with the ROSA26 reporter line to generate double heterozygous *nebl*$^{+/-}$/R26R mice in which lacZ is expressed from the ROSA26 promoter after Cre-mediated recombination.[29] E9.5 and E11.5 *nebl*$^{+/-}$/R26R embryos were fixed in 4% paraformaldehyde (PFA), and β-galactosidase staining of whole mount and transverse sections was performed as previously described.[21] Imaging was performed on a dissecting microscope (SV-6; Carl Zeiss MicroImaging, Inc.) with a 35-mm camera (C-mount; Nikon).

2.3 *In situ* hybridization

Whole-mount *in situ* hybridization of paraffin sections at different stages of mouse development was carried out using digoxigenin-labelled RNA probes as previously described.[30,31] A 718 bp RNA probe spanning bp 646–1363 of mouse nebulette XM_006497555 was utilized.

2.4 Histology, immunohistochemistry, and transmission electron microscopy

For histology and immunostaining, mouse hearts were harvested and relaxed in 50 mM KCl in PBS before overnight fixation in 4% PFA in PBS. For histology, hearts were dehydrated and embedded in paraffin, whereafter 10 μm sections were cut and analysed by staining with haematoxylin and eosin, or Picrosirius red. For immunostainings, fixed hearts were saturated in 10 and 30% sucrose in PBS and subsequently frozen in OCT, whereafter 10 μm cryosections were cut. Permeabilization and blocking were performed for 1 h in blocking solution containing 3% normal goat serum, 0.3% Triton X-100, 50 mM glycine, and 1% cold water fish gelatin (Sigma-Aldrich) in PBS after which sections were incubated with primary antibodies in wash buffer (blocking buffer diluted 10 times in PBS) overnight at 4°C. The following primary antibodies were used: nebulette (1 : 50; kindly provided by Dr Siegfried Labeit), myopalladin[26] (1 : 50), palladin 621 (1 : 100; kindly provided by Dr Carol Otey, University of North Carolina, Chapel Hill, NC, USA), N-WASP (1 : 25; Santa Cruz D15, #sc-10122), cypher [1 : 100;[32] CapZ β1 (5 μg/mL; Developmental Studies Hybridoma Bank, University of Iowa, Iowa, IA, USA (DSHB), #1E5.25.4], sarcomeric α-actinin (1 : 500; Sigma-Aldrich #A7811), desmin (1 : 80; Abcam #ab8592), filamin C (1 : 1000; kindly provided by Dr Dieter Fürst, University of Bonn, Germany), tropomyosin CH1 (5 μg/mL; DSHB, CH1), troponin T (5 μg/mL; DSHB, CT3), and tropomodulin (1 : 500; kindly provided by Dr Mark Sussman, San Diego State University, San Diego, CA, USA). After washing, sections were incubated at room temperature for 4 h with rhodamine-labelled phalloidin (1 : 100, Sigma-Aldrich) or Alexa-Fluor-488 or -568-conjugated IgG secondary antibodies (1 : 500, Life Technologies). Confocal microscopy was performed using an Olympus Fluoview FV1000 laser scanning confocal microscope with a ×60 oil immersion lens (N.A. 1.3; Olympus). Individual images (1024 × 1024) were converted to tiff format and merged as pseudocolour RGB images using ImageJ. For transmission electron microscopy (TEM), the heart was excised and fixed in 2% PFA and 2% glutaraldehyde in 0.15 M sodium cacodylate buffer, pH 7.4, as previously described.[33] Briefly, the left ventricle was cut into small pieces (~1 mm cubes) and stained overnight in 1% osmium tetroxide and 0.8% potassium ferrocyanide. The following day, tissue was stained for 2 h in 2% uranyl acetate and subsequently dehydrated in a series of ethanol and acetone washes. The tissue was embedded in Durcupan resin (EMD, Gibbstown, NJ, USA) and ultrathin sections (60–70 nm) were stained with lead citrate. Electron micrographs were recorded by using a JEOL 1200EX electron microscope operated at 80 kV. Z-line width was measured using the ImageJ 2.0.0 software based on the analysis of >100 Z-lines per heart from 2 to 3 mice per genotype and time point. Z-line values were binned in 10 nm binds and plotted in histograms fitted with the Gaussian distribution using the PRISM 6 software.

2.5 Western blot analysis

Total left ventricular tissue was homogenized in lysis buffer (50 mM Tris pH 7.5, 150 mM NaCl, 10 mM $MgCl_2$, 0.5 mM DTT, 1 mM EDTA, 10% glycerol, 2% SDS, 1% Triton X-100, Roche Complete Protease Inhibitor Cocktail, 1 mM PMSF, 1 mM $NaVO_3$, and 5 mM NaF) using a TissueLyser II (Qiagen), whereafter western blot analysis was performed using primary antibodies against the following proteins: nebulette (1 : 200), myopalladin (1 : 1000), palladin 621 (1 : 500), N-WASP (1 : 50), CapZ β1 (0.4 μg/mL), zyxin (1 : 50, Transduction laboratory no. Z45420), α-actinin (1 : 300 000), desmin (1 : 30 000), cypher (1 : 500), filamin C (1 : 10 000), tropomyosin (1 : 10 000), troponin I (0.2 ng/mL; DSHB TI-4), troponin T (2.3 ng/mL), tropomodulin (1 : 1000), CARP (1 : 50), MYL2/MLC2v[34] (1 : 5000), MYL7/MLC2a[34] (1 : 10 000), and myomesin (1 μg/mL; DSHB mMaC myomesin B4). α-Tubulin antibodies (1 : 4000; Abcam) were used for normalization.

2.6 *In vivo* cardiac physiology

For transthoracic echocardiography, mice were anaesthetized with 1% isoflurane and imaged as previously described.[35] For surgical procedures, mice were anaesthetized by an intraperitoneal injection of a mixture of ketamine (100 mg/kg) and xylazine (5 mg/kg), and the depth of anaesthesia was monitored by toe pinch. Cardiac haemodynamic parameters were evaluated by insertion of a 1.4-Fr Millar catheter-tip micromanometer catheter through the right carotid artery into the left ventricle. Pressure was recorded at baseline and following stimulation with graded doses of the β-adrenergic agonist dobutamine (0.75, 2, and 4 μg/kg/min) as previously described.[36] Transaortic constriction (TAC) was performed with a 27-gauge needle as previously described.[35] Echocardiography was performed 14 days after TAC, and the pressure gradient was measured by Doppler echocardiography. Only mice showing an adequate pressure gradient (>70 mmHg) were included in the analysis. SHAM-operated mice were used as controls.

2.7 RNA analyses

Total RNA was isolated from left ventricles of mice 3 weeks after SHAM or TAC surgery using TRIzol reagent (Life Technologies) according to the manufacturer's instructions. For quantitative RT-PCR (qRT-PCR), first-strand cDNA synthesis was performed using the High-Capacity cDNA Reverse Transcription kit from Applied Biosystems (Life Technologies), whereafter qRT-PCR was performed in triplicate with custom-designed oligos (see Supplementary material online, *Table S1*) using the SYBR Select Master Mix (Life Technologies). Relative expression analysis was performed using the $\Delta\Delta C_t$ method.

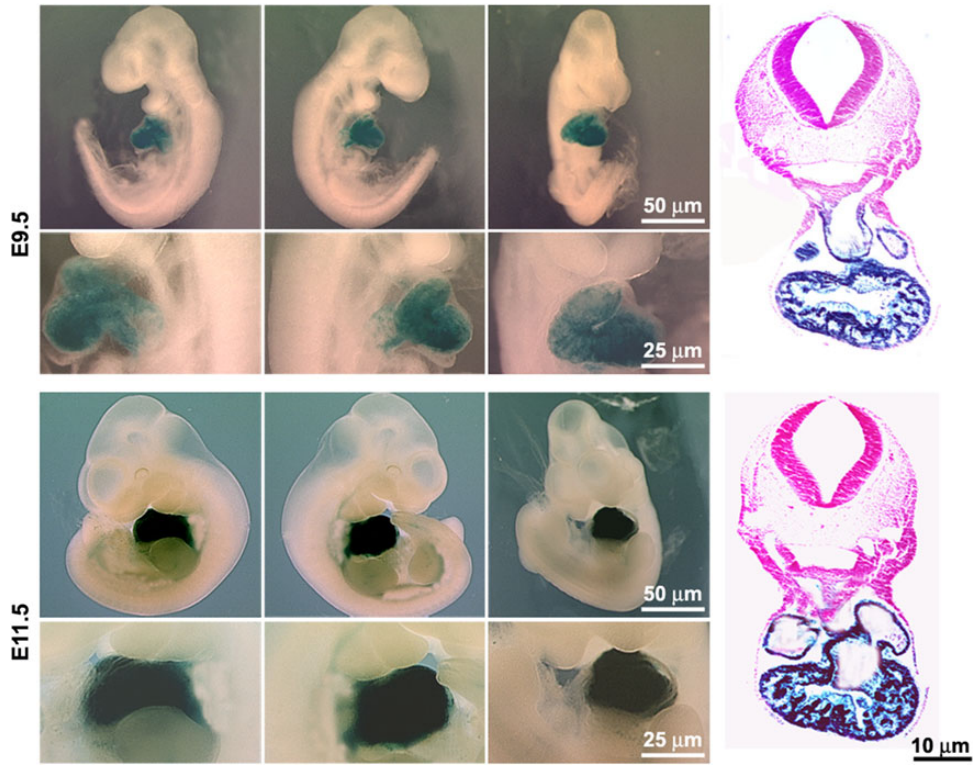

Figure 2 Lineage tracing shows specific expression of nebulette in the heart. X-Galalactosidase staining of whole mount (left, right, and centre views) and transverse sections of *nebl*$^{+/-}$/*R26R* embryos at E9.5 and E11.5.

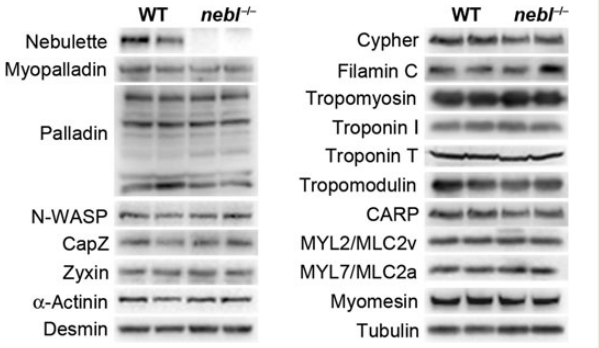

Figure 3 Western blot analysis on left ventricular lysate from WT and *nebl*$^{-/-}$ mice for various nebulette-associated and sarcomeric proteins. α-Tubulin antibody was used as a loading control. The blots are representative of at least three different experiments.

2.8 Mechanical experiments in isolated myofibrils

Mechanical experiments were performed at 15°C in single myofibrils and small bundles of a few myofibrils from frozen ventricular strips of *nebl*$^{-/-}$ and WT mice as previously described.[37] Myofibrils (30–80 μm long, 1–4 μm wide, initial sarcomere length around 2.2 μm) were mounted between a length control motor and an opto-electronic force transducer, and were maximally Ca^{2+}-activated (pCa 4.5) and fully relaxed (pCa 8.0) by fast (<5 ms) solution switching. Activating and relaxing solutions were as previously described (EGTA 10 mM, MgATP 5 mM, free Mg^{2+} 1 mM, and inorganic Pi <5 μM).[37] Maximal tension and the kinetics of force activation following rapid Ca^{2+} activation, force redevelopment following release-restretch protocols, and force relaxation following rapid Ca^{2+} removal were measured (see Supplementary material online, *Figure S3*). Quasi-steady-state sarcomere length–resting tension relations were determined in relaxing solution (pCa 8.0) for both myofibril groups. Ramp elongations of different extents (10–40% of the slack myofibril length) were applied to the preparations. Sarcomere length and resting tension were measured several seconds after each length change, when most of stress relaxation was over.

2.9 Statistical analysis

Data are presented as mean ± S.D. or S.E.M. as indicated. Statistical comparisons between WT and *nebl*$^{-/-}$ mice were done using the unpaired Student's *t*-test. A value of $P < 0.05$ was considered significant.

3. Results

3.1 Generation of nebulette KO (*nebl*$^{-/-}$) mice

To study the role of nebulette *in vivo*, nebulette KO mice (*nebl*$^{-/-}$) were generated by replacement of exon 1 by Cre under the control of the endogenous *nebl* promoter (*Figure 1A*). Targeted ES cell clones were identified by Southern blot analysis (*Figure 1B*), and the successful ablation of nebulette was confirmed by PCR and western blot analysis (*Figure 1C*). Unexpectedly, we also found a 23-fold down-regulation in mRNA levels of *lasp2* (encoding LIM and SH3 Protein-2/LIM-Nebulette),

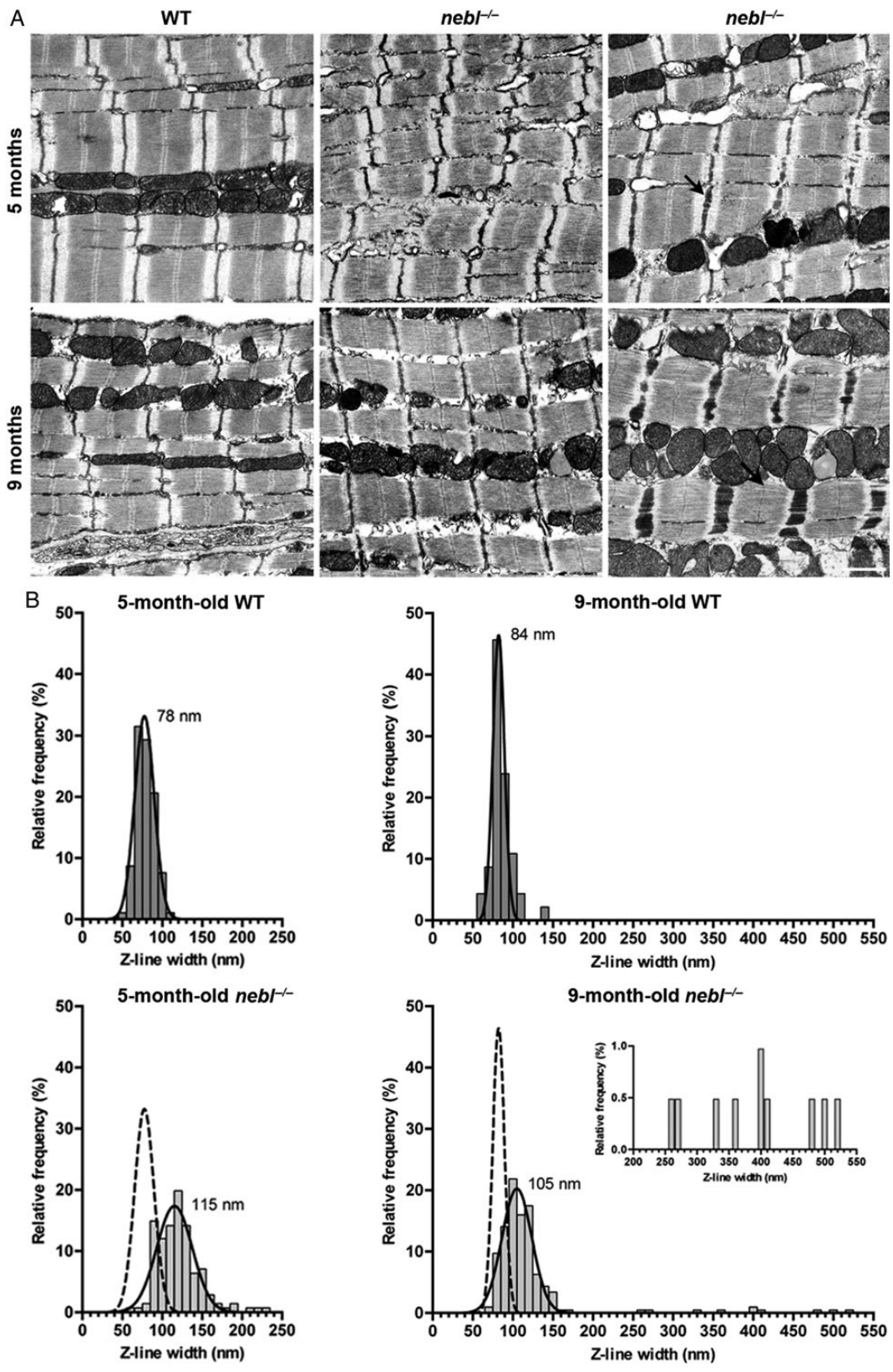

Figure 4 TEM analysis show Z-disc widening and irregularities in the left ventricle from *nebl*$^{-/-}$ mice. (*A*) Representative electron micrographs of left ventricle from 5- and 9-month-old WT and *nebl*$^{-/-}$ mice. Moderate Z-line widening was observed in *nebl*$^{-/-}$ mice and at 9 months of age, areas with severely widened Z-discs were observed. Arrows show examples of wide Z-discs. Scale bar: 1 μm. (*B*) Analysis of Z-line widths ($n \geq 100$ per heart, $n = 2–3$ per genotype, and time point). Histograms fitted with the Gaussian distribution are shown. The Gaussian fits of Z-line width in WT fibres are superimposed on the histograms from the analysis of *nebl*$^{-/-}$ fibres. The insert is a zoom-in of the Z-line measurements over 200 nm in 9-month-old *nebl*$^{-/-}$ mice.

a splice variant of nebulette transcribed from a distinct promoter[38] (*Figure 5* and see Supplementary material online, *Table S2*). While the *nebl* gene consists of 28 exons, *lasp2* is composed of only 7 exons, and encodes a protein with a domain structure significantly different from that of *nebl*, i.e. LASP2 contains a LIM domain, three central nebulin repeats, and an SH3 domain. *Lasp2* exons 5, 6, and 7 correspond to *nebl* exons 24, 27, and 28, whereas *lasp2* exons 1–4 are 5′ of *nebl* exon 1. It is possible that the replacement of *nebl* exon 1 and part of intron 1 with Cre cDNA may have affected *lasp2* splicing, leading to the dramatically decreased transcript levels of *lasp2*. *Nebl*$^{-/-}$ mice were born at Mendelian ratios, were indistinguishable from their WT littermates, and had a normal life span.

Table 1 Echocardiographic analysis of 9-month-old male *nebl*$^{-/-}$ mice compared with WT mice under basal conditions

	WT ($n = 6$)	*nebl*$^{-/-}$ ($n = 6$)
Body weight (g)	35.5 ± 2.6	33.2 ± 2.6
Heart rate (bpm)	574 ± 44	568 ± 72
LVIDd (mm)	4.03 ± 0.58	3.86 ± 0.43
LVIDs (mm)	2.54 ± 0.50	2.29 ± 0.47
IVSd (mm)	0.64 ± 0.05	0.61 ± 0.03
LVPWd (mm)	0.63 ± 0.05	0.62 ± 0.04
LV %FS	37.3 ± 3.5	41.1 ± 6.2
LVM (mg)	87.7 ± 17.2	77.9 ± 15.2
LVM/BW (mg/g)	2.47 ± 0.05	2.34 ± 0.04

All data are presented as mean ± S.D.
BW, body weight; LVIDd, left ventricular internal diameter in diastole; LVIDs, left ventricular internal diameter in systole; IVSd, interventricular septal thickness in diastole; LVPWd, left ventricular posterior wall thickness in diastole; LV %FS, left ventricular fractional shortening; LVM, left ventricular mass; bpm, beats per minute.

3.2 Lineage analysis shows specific expression of nebulette in the heart

The insertion of Cre under the control of the endogenous *nebulette* promoter allowed us to perform lineage tracing by crossing heterozygous nebulette KO (*nebl*$^{+/-}$) mice with the ROSA26 Cre reporter strain,[29] which upon Cre-mediated recombination of the R26R locus expresses lacZ, thus resulting in selective lacZ expression in nebulette-expressing cells or precursors. E9.5 and E11.5 *nebl*$^{+/-}$/*R26R* mouse embryos were stained for β-galactosidase activity, which revealed specific and homogeneous expression of nebulette in the heart in agreement with its reported localization (*Figure 2*). Consistent with these findings, whole-mount *in situ* hybridization analysis of WT embryos at E8.5, E9.5, and E11.5 revealed specific expression of nebulette in the heart (see Supplementary material online, *Figure S1*).

3.3 *Nebl*$^{-/-}$ mouse hearts have normal cytoskeletal organization, but show progressive Z-line widening

Nebl$^{-/-}$ mice had normal heart weight-to-body weight ratios and histological analyses by haematoxylin and eosin, and Picro sirius red stainings showed no cardiac abnormalities up till 8 months of age (see Supplementary material online, *Figure S2A* and data now shown). In addition, immunostainings for nebulette-associated and sarcomeric proteins showed normal cytoskeletal organization and no effects on the localization of any of the tested proteins (see Supplementary material online, *Figure S2B*). Likewise, western blot analyses on left ventricular lysate showed no changes in protein levels of various sarcomeric proteins, many of which associated with nebulette (*Figure 3*). On the other hand, TEM analysis revealed progressive Z-line abnormalities, including regions with severe Z-line widening and irregularities, in the left ventricle of *nebl*$^{-/-}$ mice compared with WT controls starting from around 5 months of age (*Figure 4A*). As evident from the

Table 2 Echocardiographic analysis of 8-week-old male *nebl*$^{-/-}$ mice compared with WT mice before and 14 days after mechanical pressure overload induced by TAC

	Before TAC		14 days after TAC	
	WT ($n = 6$)	*nebl*$^{-/-}$ ($n = 7$)	WT ($n = 6$)	*nebl*$^{-/-}$ ($n = 7$)
Age (weeks)	13.3 ± 0.0	13.3 ± 0.0	15.3 ± 0.0***	15.3 ± 0.0§§§
Body weight (g)	26.7 ± 1.1	26.1 ± 1.6	27.5 ± 0.6	26.6 ± 1.7
Heart rate (bpm)	517 ± 19	497 ± 23	461 ± 29	506 ± 12
LVIDd (mm)	3.16 ± 0.08	3.10 ± 0.17	3.07 ± 0.07	3.08 ± 0.03
LVIDs (mm)	1.63 ± 0.11	1.69 ± 0.36	1.99 ± 0.04***	2.00 ± 0.03§
IVSd (mm)	0.86 ± 0.05	0.86 ± 0.06	1.08 ± 0.03***	1.09 ± 0.02§§§
LVPWd (mm)	0.92 ± 0.02	0.88 ± 0.09	1.09 ± 0.01***	1.07 ± 0.03§§§
LV %FS	48.3 ± 3.7	49.1 ± 12.8	35.3 ± 1.2***	34.8 ± 1.4§§
LVMd (mg)	110.4 ± 18.1	101.0 ± 15.7	148.9 ± 1.8	128.1 ± 18.8
LVM/BW (mg/g)	4.14 ± 0.65	3.88 ± 0.57	5.32 ± 0.07	4.83 ± 0.70
HW/BW (mg/g)			6.01 ± 0.19	6.12 ± 0.59

Data comparison was carried out before and after TAC. See the *Table 1* legend for details and description of abbreviations.
TAC, transverse aortic constriction.
***$P < 0.001$ for WT TAC vs. WT baseline.
$^{§}P < 0.05$.
$^{§§}P < 0.01$.
$^{§§§}P < 0.001$ for *nebl*$^{-/-}$ TAC vs. *nebl*$^{-/-}$ baseline.

Table 3 Cardiac haemodynamic properties of 12-week-old male *nebl*$^{-/-}$ mice compared with WT mice at baseline and following dobutamine stimulation

	DOB	WT (n = 8)	*nebl*$^{-/-}$ (n = 8)
Heart rate (bpm)	Basal	392 ± 44	408 ± 13
	0.75 u	422 ± 33	430 ± 35
	2 u	468 ± 35	462 ± 32
	4 u	522 ± 47	510 ± 16
LVP_{max} (mmHg)	Basal	133 ± 17	122 ± 16
	0.75 u	145 ± 14	132 ± 16
	2 u	158 ± 14	143 ± 13
	4 u	158 ± 21	147 ± 11
dP/dt_{max} (mmHg/s)	Basal	10003 ± 1166	11834 ± 2576
	0.75 u	11829 ± 1532	13363 ± 2599
	2 u	16126 ± 1858	16743 ± 3087
	4 u	20464 ± 1796	20528 ± 2145
dP/dt_{min} (mmHg/s)	Basal	−8164 ± 1368	−7997 ± 1306
	0.75 u	−9559 ± 1826	−9105 ± 1317
	2 u	−12017 ± 2415	−10925 ± 1358**
	4 u	−14080 ± 2671	−13542 ± 1314
EDP (mmHg)	Basal	0.58 ± 2.31	−1.00 ± 1.02
	0.75 u	0.12 ± 1.61	−0.93 ± 1.40
	2 u	−0.34 ± 1.77	−1.00 ± 1.50
	4 u	0.02 ± 1.96	−0.50 ± 1.53
Exp. Tau (ms)	Basal	10.7 ± 1.26	11.5 ± 2.2
	0.75 u	9.6 ± 1.0	10.7 ± 1.5
	2 u	7.9 ± 0.7	9.3 ± 1.2*
	4 u	6.7 ± 0.6	7.3 ± 1.0
HW/BW (mg/g)		4.3 ± 0.5	4.0 ± 0.3

Values are mean ± S.D.
LVP_{max}, maximum end-systolic left ventricular pressure; dP/dt_{max}, maximum positive first derivative of LVP (contractility); dP/dt_{min}, maximum negative first derivative of LVP (relaxation); EDP, end-diastolic pressure; Exp. Tau, experimental Tau; DOB, dobutamine; u, units.
*$P < 0.05$.
**$P < 0.01$.

histograms in *Figure 4B*, moderately increased Z-line width was observed in the left ventricle of *nebl*$^{-/-}$ mice both at 5 and 9 months of age, while regions with severely widened Z-lines (>250 nm) were observed at 9 months of age (~5% of Z-lines). Furthermore, localized areas with an irregular Z-line were observed as shown in *Figure 4A* (top centre). The average Z-line width in WT and *nebl*$^{-/-}$ mice was 79 ± 11 and 119 ± 28 nm at 5 months of age and 85 ± 14 and 122 ± 67 nm at 9 months of age. No abnormalities in mitochondria or other organelles were observed.

3.4 *Nebl*$^{-/-}$ mice exhibit normal cardiac morphology and function both under basal conditions and in response to mechanical pressure overload

To determine the effect of nebulette KO on cardiac morphology and function, echocardiography was performed on 8-week- and 9-month-old *nebl*$^{-/-}$ mice compared with WT control mice. As shown in *Tables 1* and *2*, no significant differences were found between *nebl*$^{-/-}$ and WT mice in any of the parameters. Likewise, haemodynamic function, as assessed by cardiac catheterization of 12-week-old *nebl*$^{-/-}$ mice and WT in the absence and presence of graded doses of dobutamine, was comparable in *nebl*$^{-/-}$ and WT mice (*Table 3*). To determine the response to mechanical pressure overload, 8-week-old *nebl*$^{-/-}$ and WT mice were subjected to TAC. Pressure gradients were measured by Doppler echocardiography, and cardiac morphology and function was evaluated by echocardiography 2 weeks after the procedure. As shown in *Table 2*, *nebl*$^{-/-}$ and WT mice showed a similar cardiac hypertrophic response with a consequent reduction in fractional shortening. Thus, we conclude that ablation of nebulette has no effect on cardiac morphology and function, either at basal conditions or in response to mechanical pressure overload for up to 2 weeks.

3.5 Modulation of markers of cardiac remodelling in *nebl*$^{-/-}$ mice

To determine the potential effect of nebulette KO on cardiac gene expression under basal conditions and following mechanical stress, we performed qRT-PCR on left ventricular tissue from *nebl*$^{-/-}$ and WT mice following TAC or SHAM surgery (*Figure 5* and see Supplementary material online, *Table S2*). This revealed up-regulation of several markers of pathological cardiac remodelling in *nebl*$^{-/-}$ left ventricle, including *skeletal muscle alpha-actin* (*acta1*), *natriuretic peptide A* (*nppa/ANF*), *natriuretic peptide B* (*nppb/BNP*), *beta-cardiac myosin heavy chain* (*myh7*), and *cardiac ankyrin repeat protein/ankyrin repeat domain 1* (*ankrd1*). The highest levels of up-regulation were found under basal conditions where in particular *acta1* (22.5-fold), *nppa* (8.5-fold), and *nppb* (3.9-fold) were highly up-regulated. In addition, *nppa* (2.7-fold), *acta1* (2.2-fold), and *ankrd1* (1.9-fold) were up-regulated after TAC. *Collagen type III, alpha 1* (*col3a1*) was slightly up-regulated under basal conditions (1.4-fold), while other markers of fibrosis, such as *transforming growth factor, beta 1* (*tgfb1*) and *connective tissue growth factor* (*ctgf*), were unchanged. No changes in apoptosis-related genes [*caspase 3* (*casp3*), *B-cell CLL/Lymphoma 2* (*bcl2*), *bcl2-associated X-protein* (*bax*), and *tumour protein p53* (*tp53*)] were found. To determine whether the absence of a cardiac functional phenotype in *nebl*$^{-/-}$ mice may be due to compensation by nebulin, we performed qRT-PCR for *nebulin* (*neb*) and found a 3.4-fold up-regulation in *nebl*$^{-/-}$ mice subjected to SHAM, while no changes were found in TAC-operated mice. On the other hand, western blot analysis on left ventricular tissue lysate showed barely detectable levels of nebulin in both WT and *nebl*$^{-/-}$ mice, and IF staining showed no specific staining for nebulin in *nebl*$^{-/-}$ hearts (data not shown). This is consistent with the previously reported very low level of nebulin in the heart, where it is expressed in only a small fraction of cardiomyocytes.[21] Thus, the slight increase in *nebulin* transcript levels in *nebl*$^{-/-}$ hearts under basal conditions is unlikely to compensate for the absence of nebulette.

3.6 Sarcomere mechanics and cross-bridge kinetics are unaffected in *nebl*$^{-/-}$ hearts

To determine whether the absence of nebulette may affect sarcomere mechanics at rest and/or during contraction, we compared biomechanical properties of myofibril preparations from 1-year-old *nebl*$^{-/-}$ and WT mice. As shown in *Figure 6*, no significant differences in mean sarcomere slack length and resting sarcomere length–tension relationships were found in WT and *nebl*$^{-/-}$ myofibrils. In WT myofibrils, Ca^{2+}-activated contraction and kinetic parameters were essentially the same as those previously reported in mouse ventricular myofibrils[37] (*Table 4*). Neither maximal active tension, nor the kinetics of force generation and relaxation following rapid Ca^{2+} increase and removal,

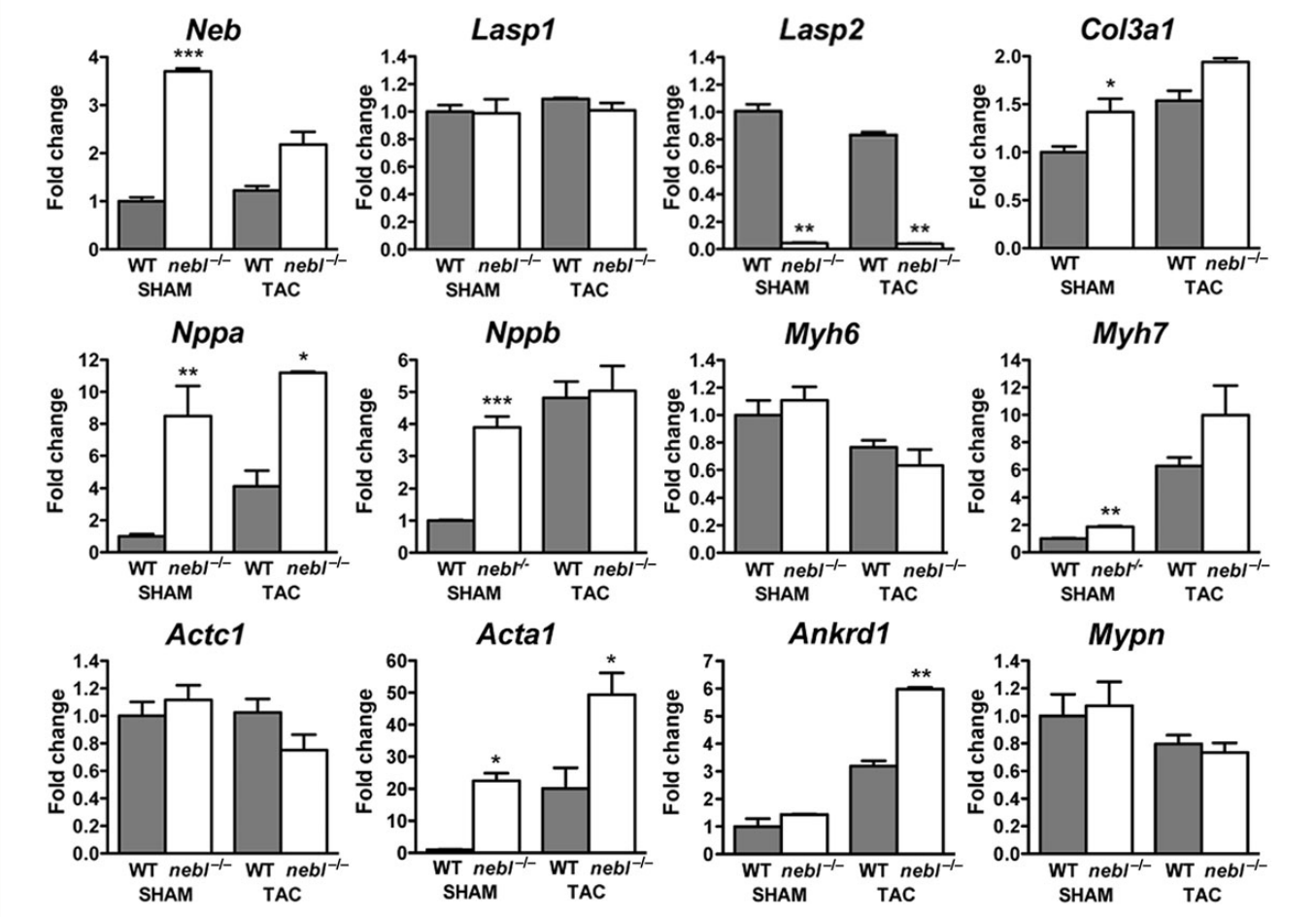

Figure 5 Up-regulation of transcript levels of *nebulin* and markers of cardiac pathological remodelling in $nebl^{-/-}$ heart. qRT-PCR analysis for *nebulin* and cardiac markers on left ventricular tissue from WT and $nebl^{-/-}$ mice 3 weeks after SHAM or TAC surgery ($n = 3$ mice per group performed in triplicate). $^{*}P \leq 0.05$; $^{**}P \leq 0.01$; $^{***}P \leq 0.001$.

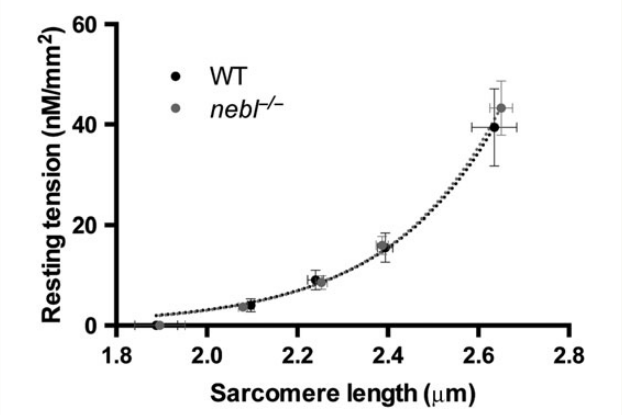

Figure 6 Average sarcomere–length resting tension relationship in myofibrils from WT and $nebl^{-/-}$ left ventricle. Each data point is mean ± S.E.M. from 5 to 15 myofibrils. Logarithmic curves are fitted to the data points.

were significantly different in WT and $nebl^{-/-}$ myofibrils. The results demonstrate that cardiac sarcomere mechanics and cross-bridge kinetics are not affected by the absence of nebulette.

4. Discussion

Although nebulette has been extensively studied *in vitro* and *nebulette* gene mutations have been associated with DCM with or without associated endocardial fibroelastosis,[27] the functional role of nebulette in the heart has remained elusive. Therefore, to provide insights into the role of nebulette *in vivo*, we generated and studied $nebl^{-/-}$ mice.

4.1 $Nebl^{-/-}$ mice exhibit no cardiac functional phenotype, but develop progressive Z-line widening and up-regulation of cardiac stress markers

Surprisingly, $nebl^{-/-}$ mice exhibited no functional cardiac phenotype or changes in myofilament function. $Nebl^{-/-}$ mice had a normal life span, even though ultrastructural analyses of the left ventricle revealed moderate Z-line widening, including areas with severely increased Z-line width, similar to observations in skeletal muscle of nebulin-deficient mice.[21] This suggests that nebulette, like nebulin,[16,21,26] is important for the maintenance of Z-line structure and integrity in cardiac muscle, although the Z-line abnormalities in $nebl^{-/-}$ mice were not sufficient to affect cardiac function. Furthermore, the presence of cardiac stress in $nebl^{-/-}$ mice is indicated by the increased expression of stress responsive genes in the left ventricle of $nebl^{-/-}$ mice both under basal

Table 4 Tension generation and relaxation in ventricular myofibrils from 1-year-old *nebl*$^{-/-}$ mice and WT mice at 15°C

Myofibril batches	Tension generation			Relaxation		
				Slow phase		Fast phase
	P_0 (mN mm^{-2})	k_{ACT} (s^{-1})	k_{TR} (s^{-1})	Duration (ms)	k_{REL} (s^{-1})	k_{REL} (s^{-1})
WT	82 ± 12 (12)	8.9 ± 0.4 (14)	8.6 ± 0.5 (14)	65 ± 6 (14)	1.79 ± 0.20 (14)	25.3 ± 3.1 (14)
nebl$^{-/-}$	83 ± 9 (14)	8.4 ± 0.6 (14)	8.4 ± 0.8 (14)	79 ± 6 (14)	1.51 ± 0.11 (15)	23.4 ± 1.9 (13)

All values are presented as mean ± S.E.M. Numbers in parentheses are the number of myofibrils.
Full tension relaxation kinetics were characterized by the duration and rate constant of tension decay of the isometric slow relaxation phase (slow k_{REL}) and the rate constant of the fast relaxation phase (fast k_{REL}; see Supplementary material online, *Figure S3*).
P_0, maximum isometric tension; k_{ACT}, rate constant of tension rise following a step-wise pCa decrease (8.0 → 3.5) by fast solution switching; k_{TR}, rate constant of tension redevelopment following release-restretch of maximally activated myofibrils.

conditions (*nppa*, *nppb*, *acta1*, and *myh7*) and following TAC (*nppa*, *acta1*, and *ankrd1*).

4.2 No changes in the expression and location of sarcomeric proteins in *nebl*$^{-/-}$ mouse hearts

Knockdown of nebulette in chicken embryonic cardiomyocytes has previously been associated with decreased thin filament length and reduced tropomyosin and troponin T along the thin filament.[7,24] In contrast, we found no changes in the expression levels and localization of tropomyosin and troponin T or any other known nebulette interaction partners in *nebl*$^{-/-}$ hearts. In particular, although N-WASP has been shown to be targeted to the Z-line through interaction with the SH3 domain of nebulin and nebulette in a GSK3β-dependent manner,[13] its localization in the Z-line was unaffected by the absence of nebulette, consistent with our recent findings in mice deficient for the nebulin SH3 domain.[26] The absent effect of nebulette KO on the expression and localization of nebulette interaction partners is in contrast to observations in transgenic mice overexpressing different DCM-associated *nebulette* mutations.[27] In these studies, depending on the overexpressed mutation, various sarcomeric proteins were found to be down-regulated (troponin T, troponin I, tropomyosin, ALP, Cypher/ZASP, α-actinin 2, and myopalladin), cleaved (filamin C and myopalladin), smeared (myopalladin and α-actinin 2), or lost from the Z-line (desmin).[27] It is unclear whether these changes are direct consequences of the mutations or indirect secondary changes as a consequence of the resulting cardiomyopathy. Also, it is possible that the non-physiological overexpression of mutant nebulette in transgenic mice may cause non-specific effects and a better model system would be to generate knockin mice for the mutations, ensuring expression at physiological levels. Nevertheless, the absence of a cardiac functional phenotype in *nebl*$^{-/-}$ mice, despite the fact that *nebulette* missense mutations have been found to result in severe DCM and endocardial fibroelastosis in both human and transgenic mouse models,[27,28] suggests that the identified *nebulette* gene mutations have dominant gain-of-function effects and could explain why no *nebulette* loss-of function mutations leading to the complete absence of nebulette have been found in DCM patients. A similar example has been observed with the myotilin KO mouse model,[39] which exhibits no phenotype, although myotilin gene mutations are causative for limb girdle muscular dystrophy 1A, myofibrillar myopathy, and spheroid body myopathy, and transgenic mice overexpressing myotilin mutations develop a myopathy phenotype.[40] Similarly, while *ankrd1* gene mutations have been described in patients with human dilated and hypertrophic cardiomyopathy,[41–43] CARP/Ankrd1 KO mice exhibit no cardiac phenotype either under basal conditions or following TAC.[43] It should also be pointed out that it is well known that differences in genetic background can influence the phenotype.[44] The *nebl*$^{-/-}$ mice were generated and analysed in a mixed sv129/Black Swiss background in our study. It is possible that *nebl*$^{-/-}$ mice may display cardiac phenotypes in a different genetic background.[45]

5. Conclusions

Although nebulette has been implicated in DCM, our results demonstrate that *nebl*$^{-/-}$ mice exhibit normal cardiac function, suggesting that nebulette is dispensable for normal cardiac function. This is in contrast to findings in nebulin KO mice, which recapitulate many of the features of nemaline myopathy.[21,46] Nevertheless, Z-line widening in *nebl*$^{-/-}$ hearts and the presence of localized areas with severe Z-line widening suggest a role of nebulette for the maintenance of Z-line integrity, similar to nebulin in skeletal muscle.[6,21,26] The absence of a functional phenotype in *nebl*$^{-/-}$ mice under basal conditions up to 9 months of age and following 2 weeks of TAC does not exclude that the *nebl*$^{-/-}$ mice may display impaired cardiac function in old age, after long-term TAC, or in response to other types of stress conditions, such as cardiac ischaemia, in particular since the up-regulation of cardiac stress responsive genes indicates the presence of chronic cardiac stress in *nebl*$^{-/-}$ mice. The fact that ablation of nebulette has no functional consequence in our study suggests that *nebulette* missense mutations, which are associated with DCM and endocardiac fibroelastosis, are not loss-of-function mutations. Further studies are needed to determine the exact mechanisms linking *nebulette* missense mutations to human cardiomyopathy.

Supplementary material

Supplementary material is available at *Cardiovascular Research* online.

Acknowledgements

The authors thank Alessandra Rodanò for the maintenance and genotyping of mice. TEM was carried out at the National Center for Microscopy and Imaging Research, University of California San Diego, La Jolla, CA, USA.

Conflict of interest: none declared.

Funding

This work was supported by grants from the National Institutes of Health, National Heart, Lung, and Blood Institute (R01-HL66100, R01-HL123626, and R01-HL106968 to J.C.); the Telethon Foundation, Italy (GGP12282 to M.L.B.); the Italian Ministry of Education, Universities and Research (PRIN 2010-2011 no. 2010R8JK2X_006 to M.L.B.); and a Transatlantic Network of Excellence grant from the Fondation Leducq (to J.C.). J.C. is the American Heart Association (AHA) Endowed Chair in Cardiovascular Research.

References

1. Wang K, Wright J. Architecture of the sarcomere matrix of skeletal muscle: immunoelectron microscopic evidence that suggests a set of parallel inextensible nebulin filaments anchored at the Z line. *J Cell Biol* 1988;**107**:2199–2212.
2. Millevoi S, Trombitas K, Kolmerer B, Kostin S, Schaper J, Pelin K, Granzier H, Labeit S. Characterization of nebulette and nebulin and emerging concepts of their roles for vertebrate Z-discs. *J Mol Biol* 1998;**282**:111–123.
3. Jin JP, Wang K. Nebulin as a giant actin-binding template protein in skeletal muscle sarcomere. Interaction of actin and cloned human nebulin fragments. *FEBS Lett* 1991;**281**:93–96.
4. Moncman CL, Wang K. Functional dissection of nebulette demonstrates actin binding of nebulin-like repeats and Z-line targeting of SH3 and linker domains. *Cell Motil Cytoskeleton* 1999;**44**:1–22.
5. Ogut O, Hossain MM, Jin JP. Interactions between nebulin-like motifs and thin filament regulatory proteins. *J Biol Chem* 2003;**278**:3089–3097.
6. Pfuhl M, Winder SJ, Pastore A. Nebulin, a helical actin binding protein. *EMBO J* 1994;**13**:1782–1789.
7. Bonzo JR, Norris AA, Esham M, Moncman CL. The nebulette repeat domain is necessary for proper maintenance of tropomyosin with the cardiac sarcomere. *Exp Cell Res* 2008;**314**:3519–3530.
8. Holmes WB, Moncman CL. Nebulette interacts with filamin C. *Cell Motil Cytoskeleton* 2008;**65**:130–142.
9. Labeit S, Kolmerer B. The complete primary structure of human nebulin and its correlation to muscle structure. *J Mol Biol* 1995;**248**:308–315.
10. Marttila M, Hanif M, Lemola E, Nowak KJ, Laitila J, Gronholm M, Wallgren-Pettersson C, Pelin K. Nebulin interactions with actin and tropomyosin are altered by disease-causing mutations. *Skelet Muscle* 2014;**4**:15.
11. Bang ML, Mudry RE, McElhinny AS, Trombitas K, Geach AJ, Yamasaki R, Sorimachi H, Granzier H, Gregorio CC, Labeit S. Myopalladin, a novel 145-kilodalton sarcomeric protein with multiple roles in Z-disc and I-band protein assemblies. *J Cell Biol* 2001;**153**:413–427.
12. Li B, Zhuang L, Trueb B. Zyxin interacts with the SH3 domains of the cytoskeletal proteins LIM-nebulette and Lasp-1. *J Biol Chem* 2004;**279**:20401–20410.
13. Takano K, Watanabe-Takano H, Suetsugu S, Kurita S, Tsujita K, Kimura S, Karatsu T, Takenawa T, Endo T. Nebulin and N-WASP cooperate to cause IGF-1-induced sarcomeric actin filament formation. *Science* 2010;**330**:1536–1540.
14. Ma K, Forbes JG, Gutierrez-Cruz G, Wang K. Titin as a giant scaffold for integrating stress and Src homology domain 3-mediated signaling pathways: the clustering of novel overlap ligand motifs in the elastic PEVK segment. *J Biol Chem* 2006;**281**:27539–27556.
15. Ma K, Wang K. Interaction of nebulin SH3 domain with titin PEVK and myopalladin: implications for the signaling and assembly role of titin and nebulin. *FEBS Lett* 2002;**532**:273–278.
16. Witt CC, Burkart C, Labeit D, McNabb M, Wu Y, Granzier H, Labeit S. Nebulin regulates thin filament length, contractility, and Z-disk structure in vivo. *EMBO J* 2006;**25**:3843–3855.
17. Pappas CT, Bhattacharya N, Cooper JA, Gregorio CC. Nebulin Interacts with CapZ and regulates thin filament architecture within the Z-disc. *Mol Biol Cell* 2008;**19**:1837–1847.
18. Bang ML, Gregorio C, Labeit S. Molecular dissection of the interaction of desmin with the C-terminal region of nebulin. *J Struct Biol* 2002;**137**:119–127.
19. Conover GM, Henderson SN, Gregorio CC. A myopathy-linked desmin mutation perturbs striated muscle actin filament architecture. *Mol Biol Cell* 2009;**20**:834–845.
20. Labeit S, Gibson T, Lakey A, Leonard K, Zeviani M, Knight P, Wardale J, Trinick J. Evidence that nebulin is a protein-ruler in muscle thin filaments. *FEBS Lett* 1991;**282**:313–316.
21. Bang ML, Li X, Littlefield R, Bremner S, Thor A, Knowlton KU, Lieber RL, Chen J. Nebulin-deficient mice exhibit shorter thin filament lengths and reduced contractile function in skeletal muscle. *J Cell Biol* 2006;**173**:905–916.
22. Castillo A, Nowak R, Littlefield KP, Fowler VM, Littlefield RS. A nebulin ruler does not dictate thin filament lengths. *Biophys J* 2009;**96**:1856–1865.
23. Pappas CT, Krieg PA, Gregorio CC. Nebulin regulates actin filament lengths by a stabilization mechanism. *J Cell Biol* 2010;**189**:859–870.
24. Moncman CL, Wang K. Targeted disruption of nebulette protein expression alters cardiac myofibril assembly and function. *Exp Cell Res* 2002;**273**:204–218.
25. Tonino P, Pappas CT, Hudson BD, Labeit S, Gregorio CC, Granzier H. Reduced myofibrillar connectivity and increased Z-disk width in nebulin-deficient skeletal muscle. *J Cell Sci* 2010;**123**:384–391.
26. Yamamoto DL, Vitiello C, Zhang J, Gokhin DS, Castaldi A, Coulis G, Piaser F, Filomena MC, Eggenhuizen PJ, Kunderfranco P, Camerini S, Takano K, Endo T, Crescenzi M, Luther PK, Lieber RL, Chen J, Bang ML. The nebulin SH3 domain is dispensable for normal skeletal muscle structure but is required for effective active load bearing in mouse. *J Cell Sci* 2013;**126**:5477–5489.
27. Purevjav E, Varela J, Morgado M, Kearney DL, Li H, Taylor MD, Arimura T, Moncman CL, McKenna W, Murphy RT, Labeit S, Vatta M, Bowles NE, Kimura A, Boriek AM, Towbin JA. Nebulette mutations are associated with dilated cardiomyopathy and endocardial fibroelastosis. *J Am Coll Cardiol* 2010;**56**:1493–1502.
28. Maiellaro-Rafferty K, Wansapura JP, Mendsaikhan U, Osinska H, James JF, Taylor MD, Robbins J, Kranias EG, Towbin JA, Purevjav E. Altered regional cardiac wall mechanics are associated with differential cardiomyocyte calcium handling due to nebulette mutations in preclinical inherited dilated cardiomyopathy. *J Mol Cell Cardiol* 2013;**60**:151–160.
29. Soriano P. Generalized lacZ expression with the ROSA26 Cre reporter strain. *Nat Genet* 1999;**21**:70–71.
30. Liang X, Zhou Q, Li X, Sun Y, Lu M, Dalton N, Ross J Jr, Chen J. PINCH1 plays an essential role in early murine embryonic development but is dispensable in ventricular cardiomyocytes. *Mol Cell Biol* 2005;**25**:3056–3062.
31. Wilkinson DG. *In Situ Hybridization: A Practical Approach*. Oxford University Press, New Year, NY, 1992.
32. Zhou Q, Chu PH, Huang C, Cheng CF, Martone ME, Knoll G, Shelton GD, Evans S, Chen J. Ablation of Cypher, a PDZ-LIM domain Z-line protein, causes a severe form of congenital myopathy. *J Cell Biol* 2001;**155**:605–612.
33. Zhang J, Bang ML, Gokhin DS, Lu Y, Cui L, Li X, Gu Y, Dalton ND, Scimia MC, Peterson KL, Lieber RL, Chen J. Syncoilin is required for generating maximum isometric stress in skeletal muscle but dispensable for muscle cytoarchitecture. *Am J Physiol Cell Physiol* 2008;**294**:C1175–C1182.
34. Kubalak SW, Miller-Hance WC, O'Brien TX, Dyson E, Chien KR. Chamber specification of atrial myosin light chain-2 expression precedes septation during murine cardiogenesis. *J Biol Chem* 1994;**269**:16961–16970.
35. Tanaka N, Dalton N, Mao L, Rockman HA, Peterson KL, Gottshall KR, Hunter JJ, Chien KR, Ross J Jr. Transthoracic echocardiography in models of cardiac disease in the mouse. *Circulation* 1996;**94**:1109–1117.
36. Arber S, Hunter JJ, Ross J Jr, Hongo M, Sansig G, Borg J, Perriard JC, Chien KR, Caroni P. MLP-deficient mice exhibit a disruption of cardiac cytoarchitectural organization, dilated cardiomyopathy, and heart failure. *Cell* 1997;**88**:393–403.
37. Kreutziger KL, Piroddi N, McMichael JT, Tesi C, Poggesi C, Regnier M. Calcium binding kinetics of troponin C strongly modulate cooperative activation and tension kinetics in cardiac muscle. *J Mol Cell Cardiol* 2011;**50**:165–174.
38. Katoh M. Identification and characterization of LASP2 gene in silico. *Int J Mol Med* 2003;**12**:405–410.
39. Moza M, Mologni L, Trokovic R, Faulkner G, Partanen J, Carpen O. Targeted deletion of the muscular dystrophy gene myotilin does not perturb muscle structure or function in mice. *Mol Cell Biol* 2007;**27**:244–252.
40. Garvey SM, Miller SE, Claflin DR, Faulkner JA, Hauser MA. Transgenic mice expressing the myotilin T57I mutation unite the pathology associated with LGMD1A and MFM. *Hum Mol Genet* 2006;**15**:2348–2362.
41. Arimura T, Bos JM, Sato A, Kubo T, Okamoto H, Nishi H, Harada H, Koga Y, Moulik M, Doi YL, Towbin JA, Ackerman MJ, Kimura A. Cardiac ankyrin repeat protein gene (ANKRD1) mutations in hypertrophic cardiomyopathy. *J Am Coll Cardiol* 2009;**54**:334–342.
42. Duboscq-Bidot L, Charron P, Ruppert V, Fauchier L, Richter A, Tavazzi L, Arbustini E, Wichter T, Maisch B, Komajda M, Isnard R, Villard E. Mutations in the ANKRD1 gene encoding CARP are responsible for human dilated cardiomyopathy. *Eur Heart J* 2009;**30**:2128–2136.
43. Meyer T, Ruppert V, Ackermann S, Richter A, Perrot A, Sperling SR, Posch MG, Maisch B, Pankuweit S. Novel mutations in the sarcomeric protein myopalladin in patients with dilated cardiomyopathy. *Eur J Hum Genet* 2013;**21**:294–300.
44. Barnabei MS, Palpant NJ, Metzger JM. Influence of genetic background on ex vivo and in vivo cardiac function in several commonly used inbred mouse strains. *Physiol Genomics* 2010;**42A**:103–113.
45. Bang ML, Gu Y, Dalton ND, Peterson KL, Chien KR, Chen J. The muscle ankyrin repeat proteins CARP, Ankrd2, and DARP are not essential for normal cardiac development and function at basal conditions and in response to pressure overload. *PLoS ONE* 2014;**9**:e93638.
46. Ottenheijm CA, Witt CC, Stienen GJ, Labeit S, Beggs AH, Granzier H. Thin filament length dysregulation contributes to muscle weakness in nemaline myopathy patients with nebulin deficiency. *Hum Mol Genet* 2009;**18**:2359–2369.